ABSTRACT

The Biochemical Characterization of a Translational Repressor.

Iron regulatory proteins (**IRP**) are crucial post-transcriptional regulators of iron metabolism. They control the synthesis of proteins involved in iron uptake, storage (ferritin) and export (ferroportin) by binding to their mRNAs. IRP1 incorporates a [4Fe-4S] cluster to double function as cytosolic aconitase (c-acon). Since RNA binding and c-acon activity are mutually exclusive, the incorporation of cluster serves as an iron-dependant regulatory switch between the two forms. This project aims to characterize the biochemical properties of IRP1 to understand the translational regulation it performs. Polysome profiles were used to isolate different forms of IRP1 based on their presence in actively translating or repressed pools of mRNA, followed by their functional characterization. Baseline activities were determined for these functional assays. Differential regulation of IRP1 on ferritin and ferroportin mRNAs was also observed. This research will allow further understanding of IRP1 as an agent of regulatory control.

Xinwei Sarah Luo / Biology

Author Name/Major

Author Signature

5/15/08

Date

Richard Eisenstein
Dept of Nutritional Sciences
Mentor Name/Department

Mentor Signature

COVER SHEET

TITLE: The Biochemical Characterization of a Translational Repressor

AUTHOR'S NAME: Xinwei Sarah Luo

MAJOR: Biology and Genetics

DEPARTMENT: Nutritional Sciences

MENTOR: Prof. Richard Eisenstein

DEPARTMENT: Nutritional Sciences

MENTOR(2): Dr. Kathryn Deck

DEPARTMENT(2): Nutritional Sciences

YEAR: 2008

The Biochemical Characterization of a Translational Repressor

Xinwei Sarah Luo

University of Wisconsin - Madison

Department of Nutritional Sciences

Summary

Iron regulatory proteins (**IRP**) are crucial post-transcriptional regulators of iron metabolism. They influence the synthesis of proteins involved in iron uptake, storage and use by binding to their mRNAs. IRP1 stands out particularly with its ability to incorporate a [4Fe-4S] cluster to double function as the enzyme, cytosolic aconitase (c-acon). Since RNA binding and c-acon activity are mutually exclusive, the incorporation of this Fe-S cluster serves as a regulatory switch between the two forms that is dependent on iron availability in cells. This project aims to characterize the biochemical properties of IRP1 in order to understand the finely tuned translational regulation it performs. Polysome profiles were used to isolate different forms of IRP1 based on their presence in actively translating or repressed pools of mRNA. Functional assays like aconitase activity assays and RNA-binding assays were used for biochemical characterization of these forms. This study establishes baseline activities for these assays and also demonstrates that IRP1 differentially regulates the mRNAs of ferritin, the iron storage protein, and ferroportin, which exports iron from the cell. My research will allow further understanding of IRP1 as an agent of regulatory control.

Introduction

Iron is required to sustain life for almost all organisms. It is found in proteins involved in the basic mechanisms of cellular respiration, DNA synthesis and cell division. It is also important for the functioning of an organism, in the transport of oxygen, immunity and brain development[1,2]. However, free iron induces the formation of reactive oxygen species which can cause damage to DNA, proteins and membranes. This dual nature of iron requires finely-tuned mechanisms of regulation which sequester excess iron but can also be induced to change when the need for iron arises. Diseases of iron metabolism arise when iron is misregulated, compelling the need for understanding iron regulation.

Various proteins are used in cells to control iron metabolism. Transferrin transports iron in blood and binds to transferrin receptor (TfR) on the surface of cell membranes. Iron is brought into the cell as a complex with TfR and is used to form iron-containing proteins[3]. The unused iron is stored in the protein ferritin. Iron can also be exported from cells via the protein ferroportin (Fpn). Iron use in the cell is regulated by modifying the synthesis rates of these proteins, which is under the control of iron regulatory proteins (IRP).

IRP are key post-transcriptional regulators of iron metabolism in cells. They bind to mRNAs of Tfr, ferritin and Fpn via sites on the mRNA called iron responsive elements (IRE) and alter their stability or translation. This regulation depends on iron availability in the cell. When the cell is iron-deficient, IRP bind to ferritin and Fpn mRNA and inhibit their translation, preventing ferritin and Fpn synthesis. When there is sufficient iron in the cell, IRP does not bind mRNA and ferritin and Fpn are synthesized to allow iron storage or export.

There are two different IRPs, IRP1 and IRP2. IRP1 is the focus of this thesis because it also functions as the enzyme cytosolic aconitase (c-acon), which converts citrate to isocitrate via

cis-aconitate in the cytosol. The c-acon form of IRP1 contains an iron sulfur [4Fe-4S] cluster in its structure. Conversion from the RNA-binding form of IRP1 to the c-acon form results from the iron-dependent incorporation of this cluster[4]. These two forms are mutually exclusive and X-ray crystallographic studies have shown that conversion from the RNA-binding form to c-acon requires a large conformational change[5,6]. Biochemical studies have also shown that a source of iron and sulfide must be available for the formation of the [4Fe-4S] cluster[3]. However, the process of cluster incorporation is still not well understood.

Previous studies have approached this fundamental question from the perspective of the aconitase form of IRP1 and asked how it loses the cluster and converts to the RNA-binding form. This project has approached it from the other direction – how the RNA-binding form incorporates a cluster and changes into the aconitase form. This project involved establishing a method for separating out the different forms of IRP1 and isolating the ribonucleoprotein fraction (RNP) – where IRP1 and its associated mRNAs are colocalized – using rat liver polysome profiles. Subsequently, biochemical characterization of these forms was done using functional assays. Measurable baseline activities for each assay were determined, thereby allowing future manipulations to be carried out.

This study also investigated the regulation of IRP1 on ferritin and ferroportin mRNAs. It is known that both contain a single IRE on the 5' untranslated region (UTR) of their mRNAs. However, it is currently unclear how IRP1 regulates the different mRNAs it binds to and by what mechanism. We observed that IRP1 differentially regulates the two mRNAs with ferritin showing greater translational repression by IRP1. By comparing the regulation of the two different mRNAs, we postulate mechanisms for IRP1 translational regulation, which will aid in better understanding of the role of IRP1 in iron metabolism.

Materials and Methods

Animals

Male Sprague-Dawley (HSD: SD) rats were used for the experiments. Study 1: Baseline measures of the various assays were obtained using a rat weighing about 500g. Study 2: This study aimed to further investigate the differential regulation of IRP1 on ferritin and ferroportin mRNA. Experiments were carried out with rats (n = 3) weighing 328 ± 7.7g, with liver weights 13.9 ± 1.8g. These rats were housed in shared cages and fed a standard diet.

All rats were acclimated to housing conditions for 1-2 weeks and subsequently killed by CO_2 asphyxiation and their livers excised for polysome profile analysis.

Polysome profile analysis of rat liver[7]

The liver of a rat was excised, washed in ice-cold polysome buffer (PB: 40 mM HEPES pH 7.4, 100 mM KCL, 5 mM MgCls, 2 mM citrate and 1 mM dithiothreitol) and minced. This was then homogenized with 1 volume of PB using a Potter Elvehjem homogenizer fitted with a Teflon pestle. The homogenate was centrifuged at 5000g for 20 min at 4°C. The upper two-thirds of the supernatant was removed and one volume of detergent (10% sodium deoxycholate and 10% Triton-X 100) was added to nine volumes of supernatant. Subsequently, 500 μL of this mixture was layered on top of an ice-cold linear sucrose gradient (11 ml, 15% to 60% sucrose in PB) which had been prepared on the same day. The gradients were centrifuged using a Sorvall TH641 swinging bucket rotor at 180,000g for 2 hours at 4°C. After centrifugation, the gradients were fractionated using an ISCO model UA-6 gradient fractionator with a chase solution of 70% sucrose in PB. The absorbance at 254 nm was measured continuously in real time. Ten fractions were collected (one every 75 seconds) and these were stored in liquid nitrogen.

RNA isolation and real time PCR of gradient fractions

RNA was isolated from 500 µL of each fraction using 750 µL of RNA STAT-60. RNA precipitation from isopropanol was carried out overnight. After isolation, the RNA was resuspended in diethylpyrocarbonate (depc)-treated water. To verify the integrity of the RNA, 2 µL of the resuspended sample was mixed with 3 volumes of formaldehyde load dye (Ambion) and run on a 1% agarose gel in TBE (100 mM Tris-borate, 2 mM EDTA, pH 8.9) containing ethidium bromide. The locations of the 18S and 28S ribosomal subunits were visualized using a UV transilluminator.

RNA concentrations and purity was determined by measuring the absorbance of a sample diluted in TE (10 mM Tris, 1 mM EDTA, pH 8.0) at 260 and 280 nm. Total cDNA from each gradient fraction was then synthesized by reverse transcription of the RNA using Superscript III reverse transcriptase (Invitrogen).

To identify the amount of ferritin, ferroportin and transthyretin mRNA present in each fraction, real-time quantitative PCR (qPCR) was done. 2X SYBR Green PCR Mastermix (Applied Biosystems) was mixed with 125 ng of cDNA and 10 µM of appropriate primers in a 25 µL reaction. The reaction was quantified using the ABI Prism® 7000 Sequence Detection System. Quantification of relative mRNA levels was done by calculating the starting fluorescence, R_0 which is proportional to the initial template quantity[8].

The primer sequences used are as follows: ferritin, left, 5'-GAATGATCCCCACTTATGTGACT-3', right, 5'-TCTTGCGTAAGTTGGTCACG-3', ferroportin, left, 5'-TGCTGCTAGAATCGGTCTTTG-3', right, 5'-GGAGTTCTGCACACCATTGA-3', and tranthyretin, sense, 5'-GGCAGCCCTGCTGTCGAT-3', antisense, 5'-TGCTGTAGGAGTACGGGC-3'.

Western blot analysis of IRP1

Total protein for each gradient fraction was quantified using the Pierce bicinchronic acid (BCA) protein assay. SDS-polyacrylamide gel electrophoresis (PAGE) was used for IRP1 quantification. For fractions containing more than 1.25 mg/ml of protein, a constant amount (25 μg) of protein was loaded onto an 8% polyacrylamide gel. For fractions containing less than 1.25 mg/ml of protein, a constant volume of protein was loaded. After separation on the gel, the proteins were transferred to a nitrocellulose membrane. IRP1 was detected using monoclonal antibody against IRP1 from mouse ascites coupled to immunofluorescent goat anti-mouse horseradish peroxidase.

Aconitase assay

To assay for the presence of the cytosolic aconitase form of IRP1, which converts citrate to isocitrate via cis-aconitate, aconitase activity was measured. A 10 μL sample of each fraction was diluted in 500 μL of aconitase assay mix (Tris pH 8.0, 20 mM DL-isocitrate) and the absorbance was continuously measured at 240 nm to detect the formation of cis-aconitate. Reconstitution assays were carried out to analyze what factors were needed to reconstitute aconitase activity from RNA-bound IRP1 or other IRP1 pools. Some samples were given Fe^{2+}, S^{2-} and a reducing agent (dithiothreitol, DTT) while others only received Fe^{2+} and a reducing agent. S^{2-} was delivered using the NifS protein that catalyzes the formation of elemental sulfur and L-alanine from the substrate L-cysteine. Dithiothreitol (DTT) was added to reduce S^0 to S^{2-}. These manipulations were done in an anaerobic chamber and aliquots were taken out at 15 min time points to analyze for aconitase activity.

RNA binding assay

This assay measures the amount of IRP1 that does not contain the Fe-S cluster and can bind mRNA. 5 µg of protein from each fraction was mixed with a 1 nM ^{32}P-labeled RNA of known radioactivity that contains IRE. An identical set of samples was treated with 2-mercaptoethanol (2ME), which causes dissociation of the Fe-S cluster. The samples were incubated for 10 min at room temperature then run on a nondenaturing 30% polyacrylamide gel in TBE. IRP1-bound RNA was separated from free RNA and quantification was done by phosphorimaging using a [^{32}P] RNA standard curve.

Micrococcal nuclease treatment

Rat liver cytosol with known DNA concentrations was incubated at 37°C with micrococcal nuclease (NEB), micrococcal nuclease reaction buffer (50mM Tris-HCl, 5mM $CaCl_2$, pH 7.9) and 100 µg/ml BSA. After 15 min incubation, the enzyme was inactivated using excess EGTA. Then, the RNA binding assay (above) was carried out with the samples containing a constant amount (7 µg) of protein.

Results

Study 1: Sucrose gradient centrifugation of the liver post-mitochondrial supernatant resulted in sedimentation of the different forms of IRP1 according to their molecular weights. Free IRP1 and the aconitase form of IRP1 were located in the earlier part of the fraction while IRP1 that is still bound to mRNA migrated further down the gradient. Polysomes, actively translating mRNA that is bound to ribosomes, migrated the furthest down the gradient (fig 1a).

Functional assays were carried out to biochemically characterize the different forms of IRP1 isolated after fractionation of the sucrose gradient. Western blots were done to determine

the level of IRP1 protein in each fraction (fig. 2b). Real-time quantitative PCR was carried out on each fraction to determine the relative ferritin, ferroportin and transthyretin (a non-iron regulated control mRNA) mRNA levels in each fraction (fig. 3). The ribonucleoprotein fraction on the gradient was determined to be where IRP1 and ferritin and ferroportin mRNA colocalize, in fractions 2 and 3. The distribution of transthyretin mRNA shows that the accumulation of ferritin and ferroportin mRNA in the earlier fractions was not due to the mRNA being degraded.

An unexpected result was the difference in distribution across the gradient for ferritin and ferroportin mRNA. For ferritin, more mRNA was found in the earlier fractions (1-4) while for ferroportin, more mRNA was found in the later fractions (5-10). Since the mRNA in earlier fractions are translationally repressed by IRP1 while those in the later fractions are translationally active, IRP1 seems to regulate these two mRNAs differently. Study 2 was carried out to further investigate this result.

The activity of c-aconitase in each fraction was measured to determine the relative amount of IRP1 that contain cluster and have aconitase activity. The distribution of aconitase activity across the gradient correlated with the distribution of IRP1 across the gradient (fig. 2b, fig. 4a). Earlier fractions contained more IRP1, presumably the free protein, which correlated with the high aconitase activity.

RNA-binding activity of IRP1 was also measured to determine the relative level of IRP1 in the RNA-binding form (fig. 4b). However, the results of this assay were more difficult to interpret. Some IRP1 might still have endogenous mRNA-bound to them and hence are not free to bind the RNA given in the reaction. There might also be some IRP1 that originally had endogenous mRNA bound but which became unbound during the experiment. The reaction only

measures IRP1 that are free to bind added RNA. Hence, this might lead to underestimation of the amount of IRP1 in the RNA-binding form.

To remove the ambiguity in this assay, we attempted to first degrade any endogenous mRNA present using micrococcal nuclease (MN) treatment, and then carry out the RNA-binding reaction. MN requires the presence of Ca^{2+} for degradation of mRNA. After MN treatment, the nuclease can be inactivated by removing the Ca^{2+} using excess EGTA so MN does not degrade the RNA probes added in the RNA-binding reaction. This treatment was first tried on rat liver cytosol but the samples with prior MN treatment showed less RNA-binding activity than control samples (fig. 5). The results from this experiment were thus inconclusive and more work is necessary to work out the parameters.

Study 2: To further investigate the differential regulation of IRP1 on ferritin and ferroportin mRNA, the qPCR and western blot experiments were repeated with another three rats each weighing about 300g. The average distribution of IRP1 from these rats was similar to that from study 1, with fraction one containing about 50% of total IRP1 (fig.6). The mRNA distributions again showed ferritin having relatively more mRNA in the earlier fractions while ferroportin had more mRNA in the later fractions (fig.7). When the relative amounts of mRNA from fractions 1-4 (repressed mRNA) and fractions 5-10 (translated mRNA) were summed, the difference between ferritin and ferroportin mRNA were statistically significant ($p<0.05$) (fig.8).

Aconitase assay was also carried out with one set of fractions from one of the rats (fig. 9). The results were largely similar to the aconitase assay results in study 1, with higher aconitase activities seen in the earlier fractions while the later fractions had barely detectable activities.

Discussion

Isolation and characterization of mRNA-bound IRP1

The ribonucleoprotein (RNP) fraction containing the mRNA-bound IRP1 localizes to the fractions on the sucrose gradient where ferritin and ferroportin mRNA levels peak and colocalize with the presence of IRP1. This was determined to be in fractions 2 and 3. In these fractions, both aconitase and RNA-binding activities were observed in the absence of treatments, which provide a good baseline measure for future manipulations. The sucrose gradient method of mRNA-bound IRP1 isolation was generally effective but fine separation between free IRP1 and mRNA-bound IRP1 was difficult to achieve. This was because individual fractions do not take into account gradations of IRP1 levels across the sucrose gradient. A gel filtration column which separates proteins based on size might enhance separation and might allow more sample to be obtained so further manipulations can be carried out. By selecting a specific pore size which allows retention of free IRP1 but exclusion of mRNA-bound IRP1, a more clear-cut separation could be achieved.

Differential regulation of ferritin and ferroportin mRNAs by IRP1

Ferritin and ferroportin mRNAs show different distributions across the gradient even though they are both regulated by IRP1 on the iron responsive element on the 5' UTR of their mRNAs. Ferritin mRNA is more repressed, with more mRNA in the earlier fractions than the later ones while the converse is true for ferroportin. Thus, IRP1 seems to regulate these two mRNAs differently. We postulate two hypotheses for this: 1) IRP1 has a higher affinity for ferritin IRE and binds it more efficiently than ferroportin IRE; 2) When IRP1 is bound to ferroportin IRE, this complex is more sensitive to iron levels than when IRP1 is bound to ferritin

IRE. Thus, the ferroportin IRE-IRP1 complex dissociates more readily in response to changing iron levels in the cell as compared to the ferritin IRE-IRP1 complex.

Studies have shown the various mRNAs that IRP1 regulates are arranged in a hierarchy, whereby IRP1 has different affinities for different IREs on the mRNAs (J. Goforth, unpublished results). Ferritin is higher up in the hierarchy than ferroportin, which corroborates with the first hypothesis that IRP1 has a greater affinity for ferritin IRE.

To further investigate the factors necessary for [4Fe-4S] cluster incorporation, future work will involve trying different manipulations on existing assays. After working out the parameters for successful mRNA degradation, the micrococcal nuclease (MN) treatment could be used with the RNA-binding assay as well as the aconitase assay. With prior MN degradation of endogenous mRNA, the reconstitution assays can also be carried out to specifically examine whether the RNA-binding form of IRP1 requires Fe or S to incorporate the [4Fe-4S] cluster.

Figures

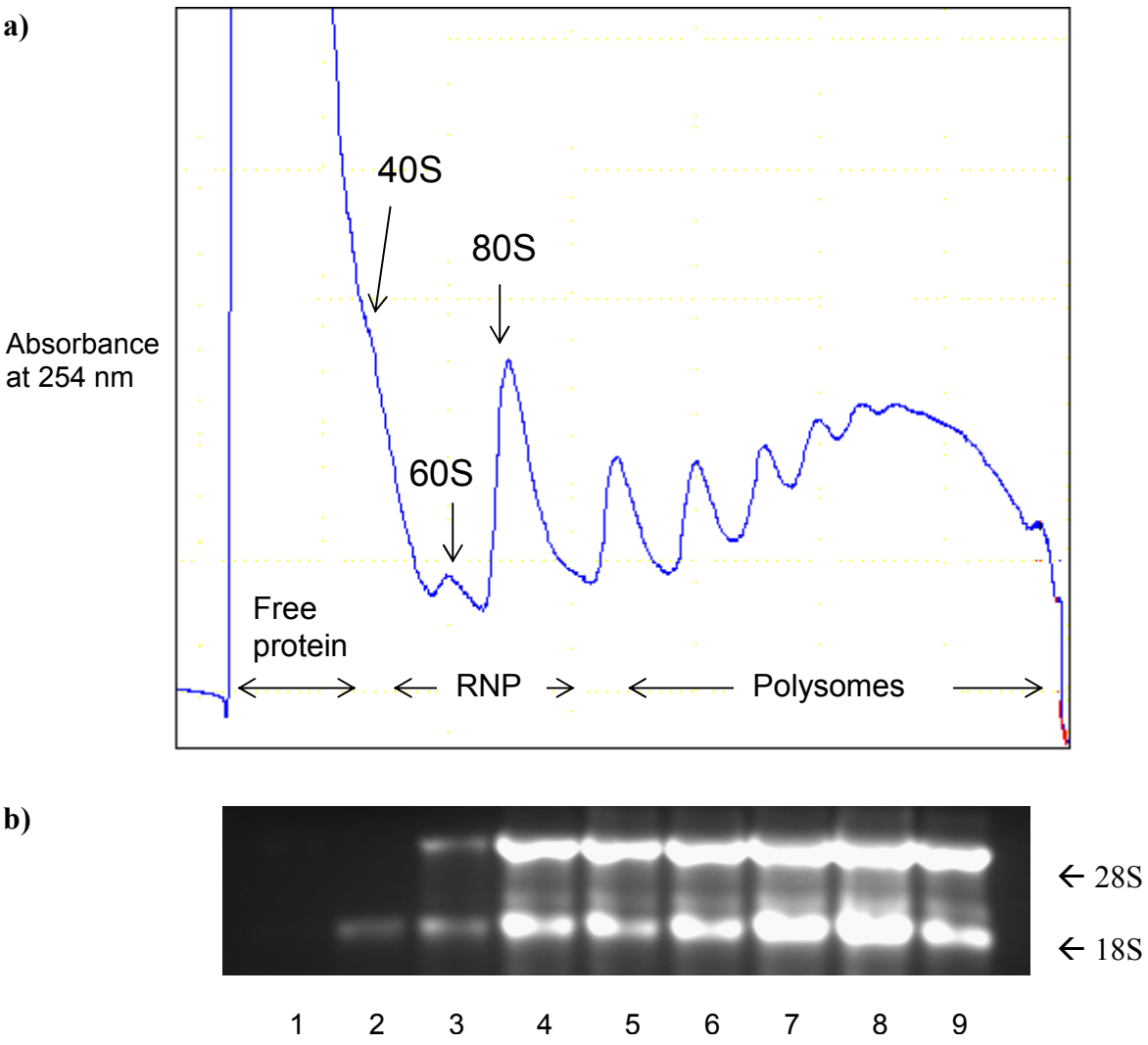

Figure 1a: Polysome Profile. Post-mitochondrial supernatant from rat liver was layered on a linear sucrose gradient, centrifuged and fractionated as outlined in Methods. The 40S and 60S ribosomal subunits and 80S monosome peaks are shown. The approximate free protein, ribonucleoprotein (RNP) and polysome regions are also indicated. Free protein is the least dense and accumulates at the top of the gradient (left) while polysomes migrate to the bottom (right).

Figure 1b: Agarose RNA gel. RNA was isolated from each fraction as described in Methods and run on a 1% RNAse-free TBE agarose gel to verify integrity. Locations of the 18S and 28S ribosomal subunit are shown. Fractions 1-2 contain free protein and some RNP. Fractions 3-4 contain RNPs, the ribosomal subunits and the 80S ribosome. Fractions 5-10 contain polysomes.

Study 1

a)

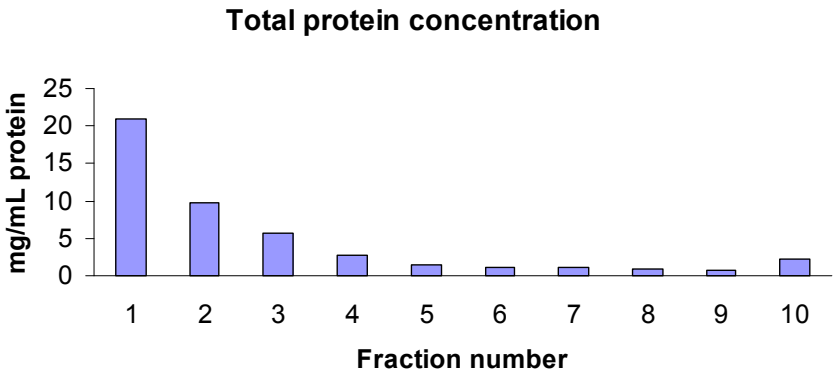

b)

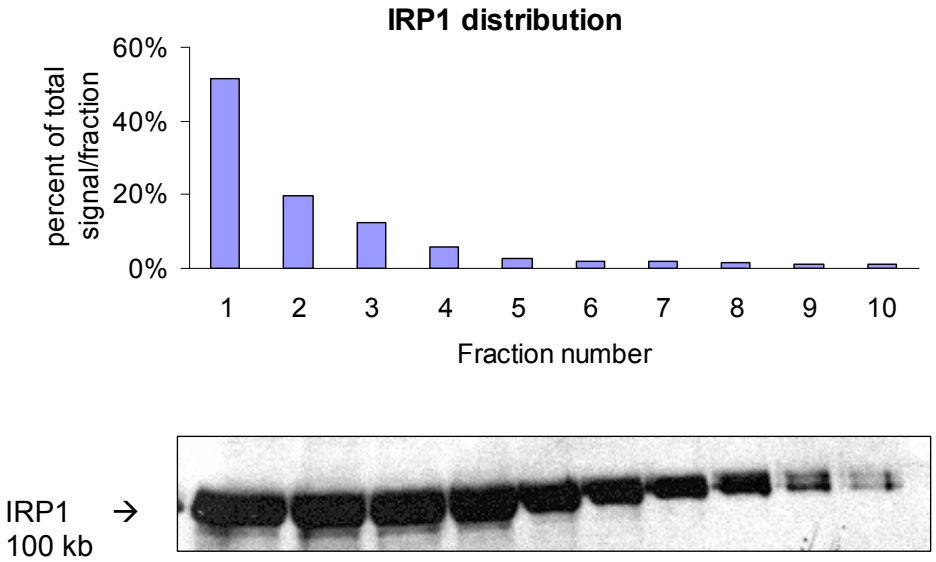

Figure 2a.

Distribution of total protein concentration across the sucrose gradient. The BCA assay was carried out with a 5 µL sample from each fraction and quantified using a bovine serum albumin (BSA) standard curve after absorbance was measured at 562 nm.

Figure 2b.

Distribution of IRP1 expression from western blot analysis. Samples from each fraction were run on an SDS gel and transferred to a nitrocellulose membrane as described in Methods. For fractions 1-4, a constant amount of 25 µg of protein was loaded and for fractions 5-10, a constant volume of protein was loaded.

Study 1

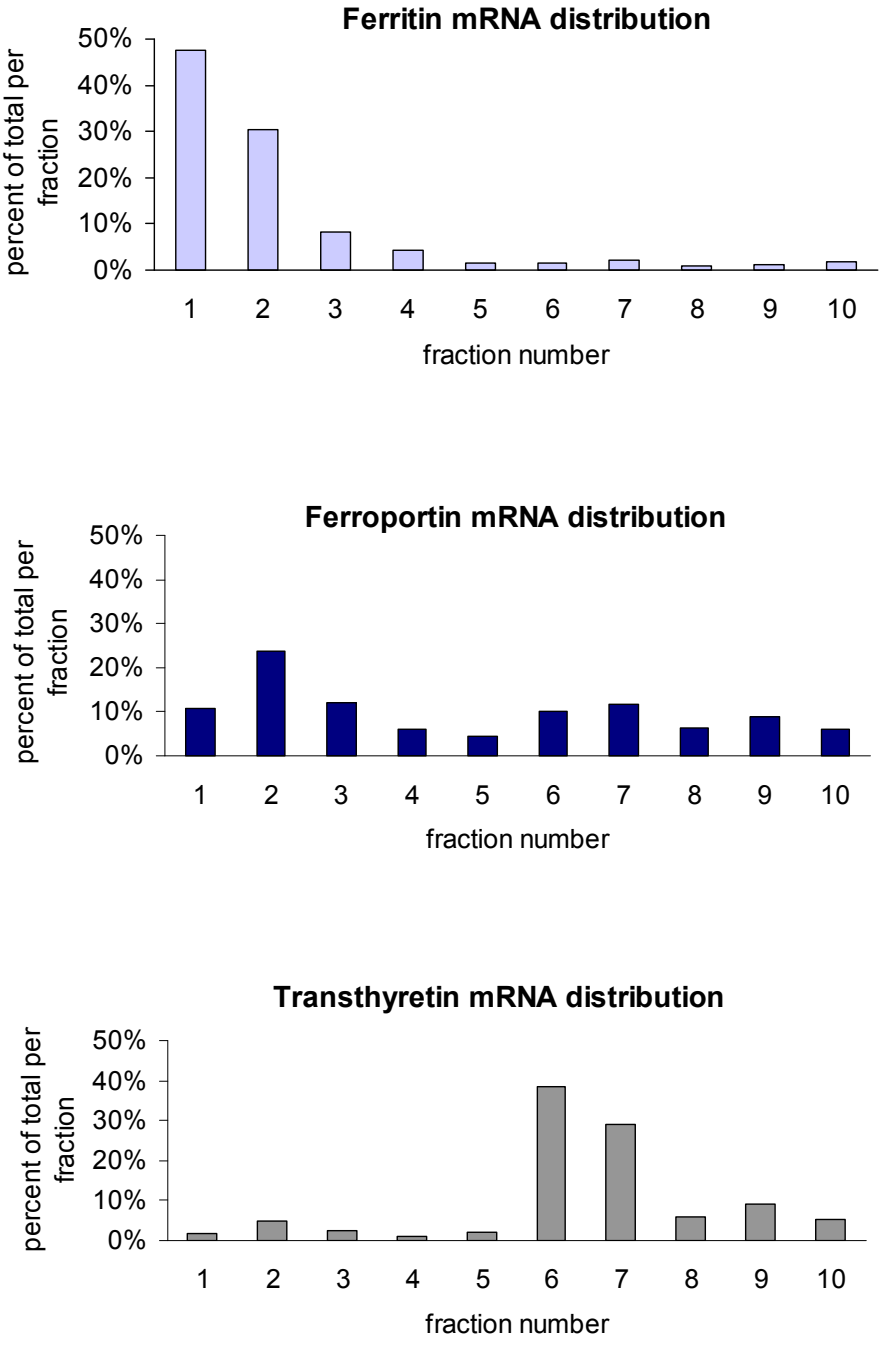

Figure 3: Distribution of percent total mRNA. Relative distributions of ferritin, ferroportin and transthyretin mRNA across the gradient were obtained by RNA isolation from each fraction followed by real-time quantitative PCR using specific primers.

Study 1

a)

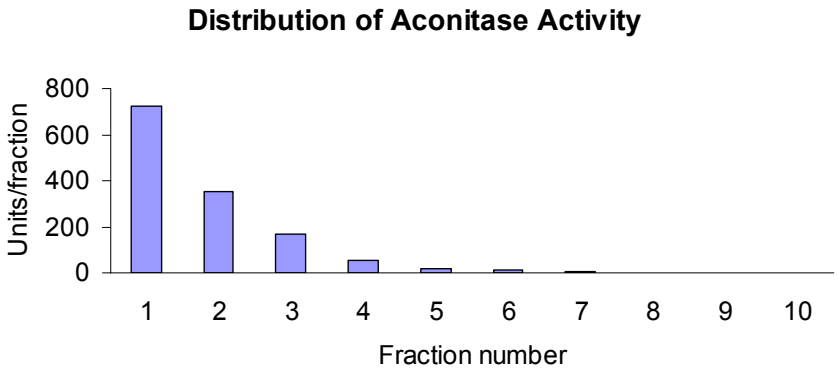

b)

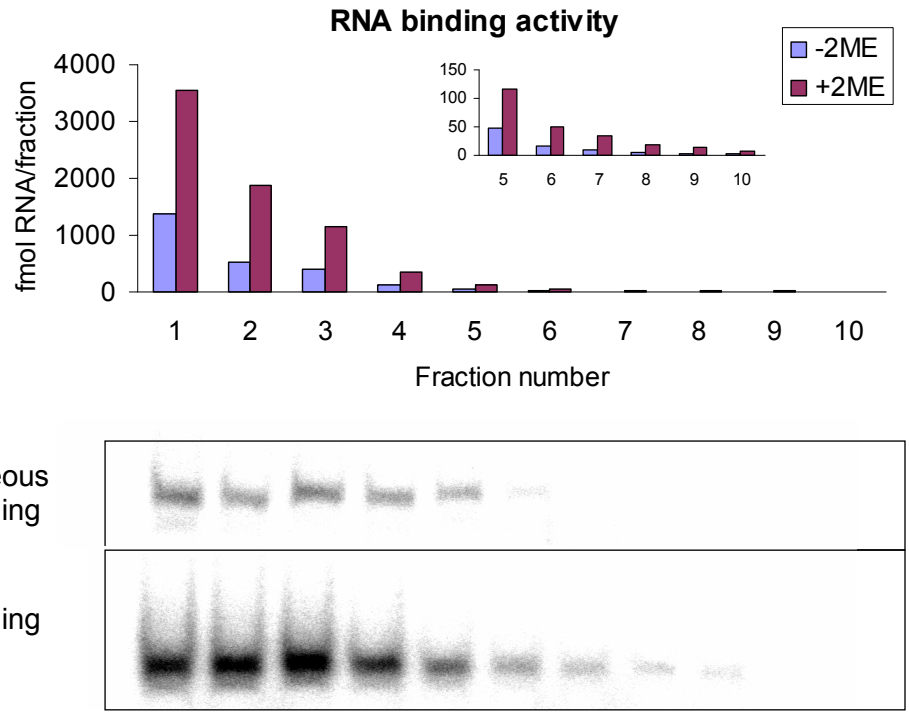

Figure 4a: Distribution of aconitase activity. A 10µL sample from each fraction was diluted in 500µL of assay mix (Tris pH 8.0, 20 mM DL-isocitrate) and the absorbance was measured continuously at 240 nm to detect formation of cis-aconitate from isocitrate.

Figure 4b: Distribution of RNA-binding activity. Samples from each fraction were mixed with ^{32}P-labeled RNA containing IRE and run on a nondenaturing polyacrylamide gel as described in methods. 2-mercaptoethanol (2ME) addition causes dissociation of cluster from c-acon, resulting in increased RNA-binding activity.

Study 1

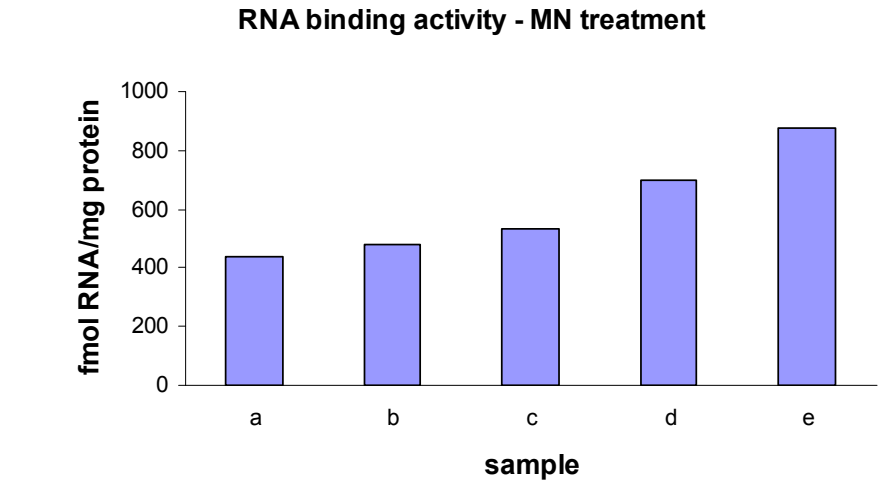

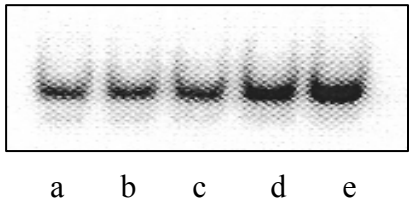

a. Incubation at 0°C
b. Incubation at RT
c. Incubation at 37°C
d. EGTA added prior to MN addition. 37°C incubation.
e. No MN added.

Figure 5: Micrococcal nuclease experiment with rat liver cytosol. Equal volumes of micrococcal nuclease (MN) were added to samples of rat liver cytosol except sample (e). Each sample was incubated for 15 min at the temperature stated above. EGTA was added to inactivate the nuclease. The RNA-binding assay was then carried out as described in Methods.

Study 2

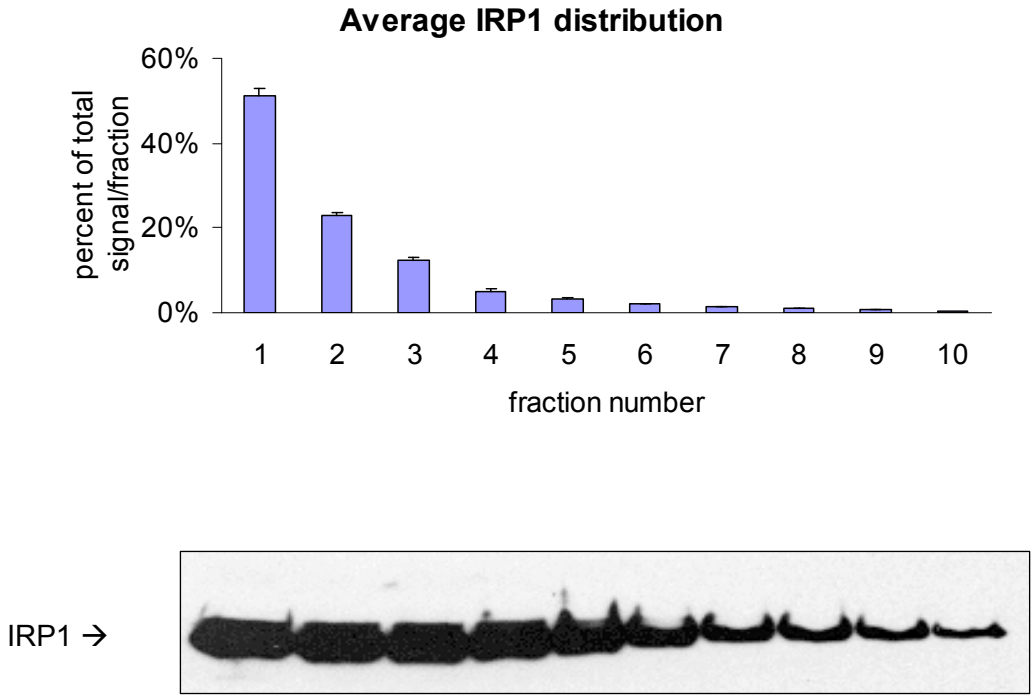

Figure 6.

Averaged IRP1 distribution for three rats. Polysome profiles of each rat were obtained as before. Western blot analysis was done on each fraction as described in Methods. For fractions 1-4, a constant amount of protein was loaded on the SDS polyacrylamide gel. For fractions 5-10, constant volumes of protein were loaded. Results are expressed as mean ± standard error of the mean for n = 3 rats.

Study 2

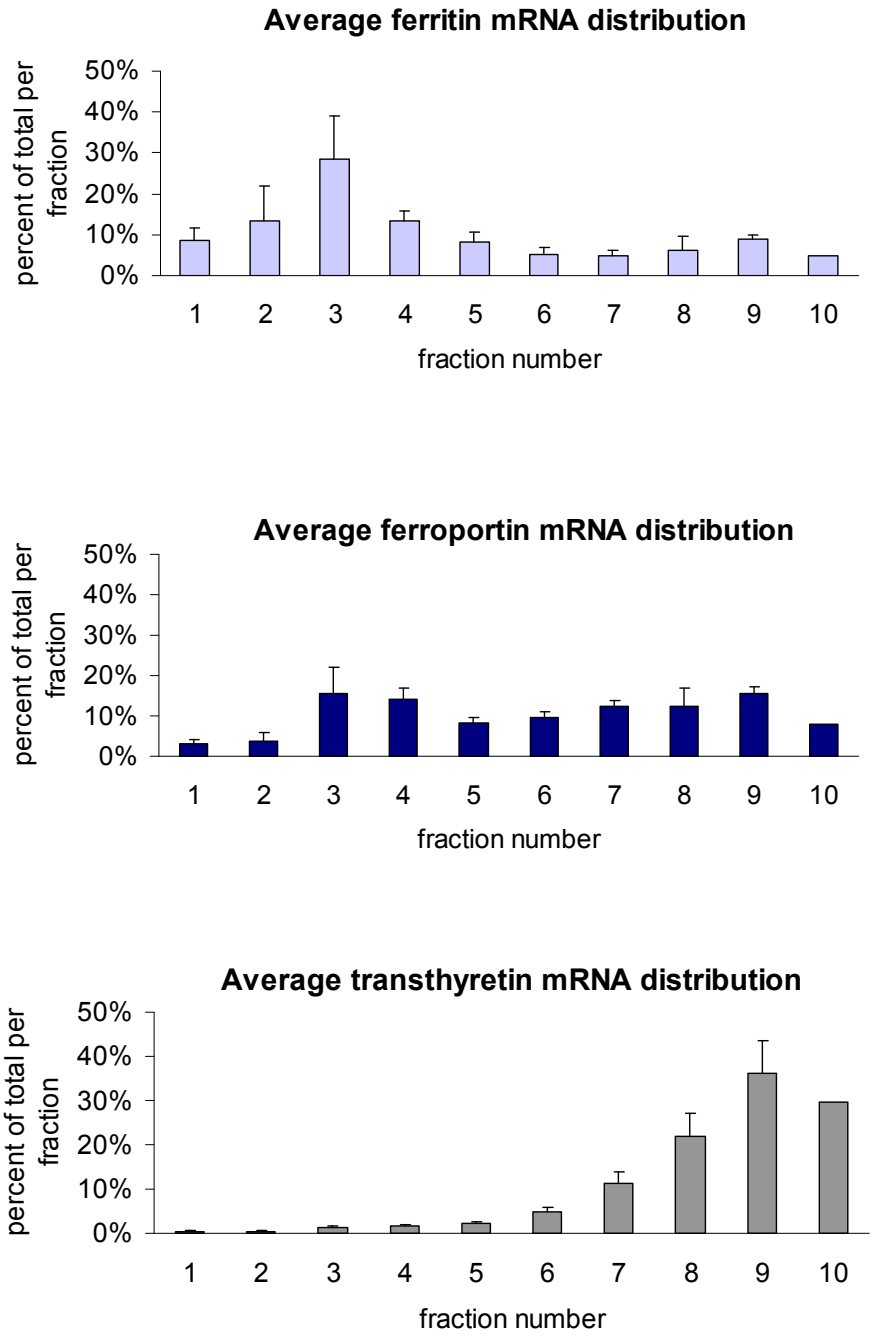

Figure 7: Averaged mRNA distributions for three rats. RNA isolation was carried out on each fraction as before and real-time quantitative PCR was performed as described in Methods. Results are expressed as mean ± standard error of the mean for n = 3 rats.

Study 2

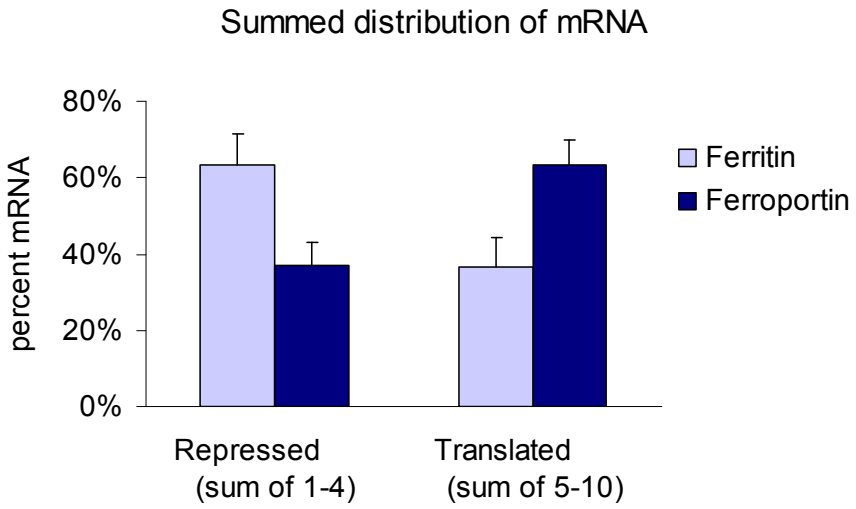

Figure 8: Summed distribution of ferritin and ferroportin mRNA in the repressed and actively translated fractions. Statistical analysis using two-tailed Student's T test showed that differences between ferritin and ferroportin mRNA in the repressed and translated pool were statistically significant ($p<0.05$). Results are expressed as mean ± standard error of the mean for n = 3 rats.

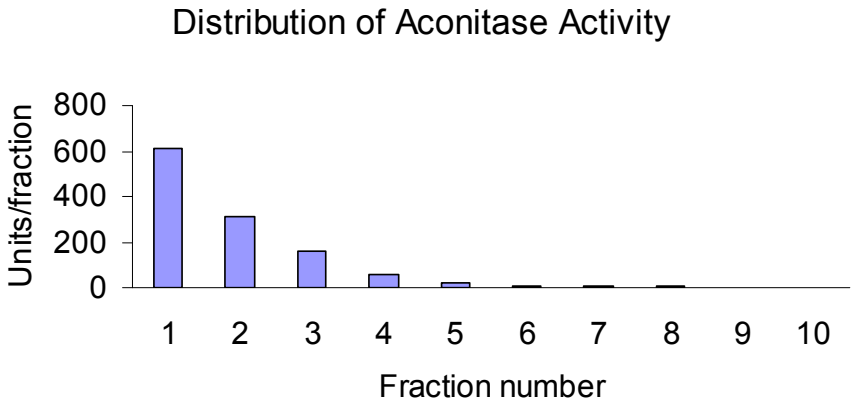

Figure 9: Distribution of aconitase activity for one rat in study 2. The experimental parameters were identical to the aconitase experiment in study 1. Distribution of aconitase activity was largely similar, with higher activity observed in the earlier fractions and almost no activity in the later fractions.

References

[1] Lieu, PT. et al. (2001) *Mol Aspects Med* 22: 1-87

[2] Beard, JL. Connor, JR. (2003) *Annu Rev Nutr* 23: 31-58

[3] Wallander ML. et al (2006) *Biochimica et Biophysica Acta* 1763: 668-689

[4] Eisenstein, RS. et al. (1997) *Metal Ions in Gene Regulation* Chapman and Hall, NY

[5] Basilion, JP. et al. (1994) *Proc. Natl. Acad. Sci* USA 91, 574-578

[6] Walden, WE. et al. (2006) *Science* 314: 1903-1908.

[7] Ross, KL. (2002) (Doctoral dissertation, University of Wisconsin-Madison)

[8] Peirson, SN. et al. (2003) *Nucl. Acids Res.,* 31(14)